

# Lithiated manganese oxides as a cathode for lithium batteries

Hiroyoshi Nakamura<sup>\*</sup>, Koichi Motooka, Hideyuki Noguchi, Masaki Yoshio

*Department of Applied Chemistry, Saga University, Saga 840-8502, Japan*

## Abstract

Lithiated manganese oxides (orthorhombic (I)) have been prepared by the heat treatment of  $\text{MnO}_2$  with  $\text{LiI}$  at 150–200°C. Highly lithiated  $\text{MnO}_2$ ,  $\text{Li}_{0.50}\text{MnO}_2$ , is obtained by using  $\text{LiI}$  as the Li source, in comparison with  $\text{Li}_{0.33}\text{MnO}_2$  obtained from  $\text{LiNO}_3/\text{MnO}_2$  mixture heated at 320–360°C. The first theoretical capacities of the orthorhombic (I),  $\text{Li}_{0.5}\text{MnO}_2$ , approximately correspond to the experimental values. The structure of the battery active material is essentially the same as  $\text{Li}_{0.33}\text{MnO}_2$ . The excellent rechargeable capacity is roughly 250 mA h/g when cycling between 4.5 and 2.0 V. By the chemical and the XRD analysis, it has been found that the orthorhombic phase (II) is formed at the initial molar ratio greater than  $\text{LiI}/\text{MnO}_2 = 1.3$  and  $\text{Li}_2\text{MnO}_3$  is formed at the heating temperature greater than 250°C. © 1999 Elsevier Science S.A. All rights reserved.

*Keywords:* Lithium batteries; Cathode material; Lithium manganese oxide

## 1. Introduction

One of the well known 3 V cathode materials for a rechargeable lithium battery would be CDMO (composite dimensional manganese oxide), which was developed and named by a Sanyo group [1,2]. CDMO was synthesized from the reaction of  $\text{LiOH}$  with EMD (electrolytically prepared manganese dioxide) in a 3:7 molar ratio heated at 370°C. Based on the XRD analysis, it contains domains of  $\gamma\text{-MnO}_2$  and the rocksalt structure  $\text{Li}_2\text{MnO}_3$ . However, its real crystal structure such as crystal system and cathode active compounds for lithium batteries is still unknown. Later, de Kock et al. [3] reported that this compound was characterized as an intergrowth structure containing a lithiated  $\gamma\text{-MnO}_2$  phase (structure of EMD) and a spinel-related phase as an impurity. If we assumed that the real cathode active material would be lithiated  $\gamma\text{-MnO}_2$ , the rechargeable capacity of EMD is around 130–140 mA h/g, whose rechargeable reaction would be the following:  $\text{Li}_{0.5}\text{MnO}_2 + 0.5\text{Li}^+ + 0.5\text{e}^- = \text{LiMnO}_2$  (theoretical capacity is 150 mA h/g in 3 V region). Thus, we have been studying to clarify the difference between the battery performance. To solve this problem, we have found that the real battery active material is  $\text{Li}_{0.33}\text{MnO}_2$ .

We have proposed the melt-impregnation method for the preparation of Li–Mn–O compounds as a cathode for lithium batteries [4–8]. This method is fundamentally a two-step heating method. It consists of first heating to the melting point of the lithium salts and then heating at the desired temperature. The advantage of this method is that the melted  $\text{LiNO}_3$  can be impregnated into the pores of the  $\text{MnO}_2$ . This makes it possible to form a Li–Mn–O compound with a single phase structure at a low temperature. We have named the heated compound of  $\text{LiNO}_3/\text{MnO}_2$  with a 1:3 molar ratio as  $\text{Li}_{0.33}\text{MnO}_2$  [4–7] (or  $\text{LiMn}_3\text{O}_6$  in the first paper [4]) having a orthorhombic structure, which is first prepared at 260°C and then heated at 320–360°C depending on the manganese dioxide used. Our novel compound is not a lithiated  $\gamma\text{-MnO}_2$ , because its rechargeable capacity is usually greater than 200 mA h/g as a 3-V cathode material and its battery reaction would be shown as  $\text{Li}_{0.33}\text{MnO}_2 + 0.66\text{Li}^+ + 0.66\text{e}^- = \text{LiMnO}_2$  (theoretical capacity is 210 mA h/g). The excellent battery performance of our  $\text{Li}_{0.33}\text{MnO}_2$  has been confirmed by Li and Pistoia [9] and successfully applied to AA-size rechargeable lithium cells using a sophisticated electrolyte that overcomes safety problems developed by Dan et al. [10] and Revi et al. [11].

In the present paper, we have tried to synthesize lithiated manganese oxides using  $\text{LiI}$  as a lithium source

<sup>\*</sup> Corresponding author

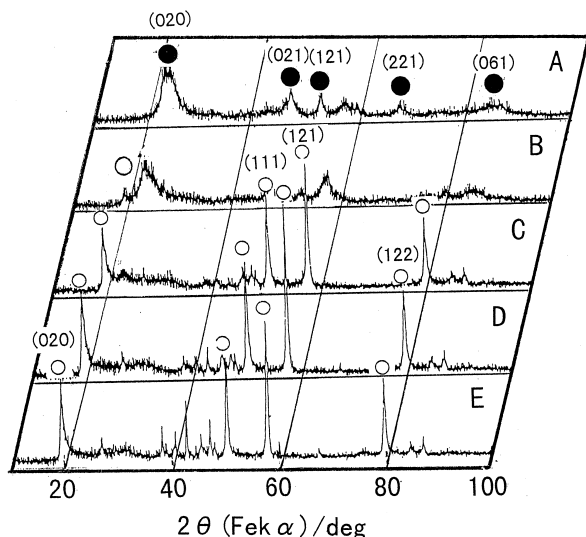


Fig. 1. XRD patterns of reaction products obtained from LiI reacting with  $\text{MnO}_2$  heated at  $200^\circ\text{C}$  with initial molar ratio of  $\text{LiI}/\text{MnO}_2$ : (A) 1, (B) 1.3, (C) 1.6, (D) 1.9, (E) 2.3. ●: Orthorhombic phase (I); ○: orthorhombic phase (II).

instead of  $\text{LiNO}_3$ , which makes it possible to heat at a lower temperature. The obtained compounds also show an orthorhombic structure, but the lithiation level is higher than  $\text{Li}_{0.33}\text{MnO}_2$ .

## 2. Experimental

Lithiated manganese oxides were prepared by heating the mixture of LiI and  $\text{MnO}_2$  (CMD-U, Chuo Denki, Kogyo, Japan) in the range of initial molar ratios of  $\text{LiI}/\text{MnO}_2 = 1\text{--}2.3$  at  $150\text{--}300^\circ\text{C}$ . After heating, the products were washed three times with hot water to remove any unreacted LiI and then dried at  $120^\circ\text{C}$ . The crystal structure were characterized using a Rigaku RINT 1000 X-ray diffractometer with  $\text{FeK}\alpha$  radiation. The Mn valence in the lithiated manganese oxides was calculated by analysis of the total manganese and oxidation power of the Mn ion according to EDTA titration and oxidation–reduction titration using  $\text{KMnO}_4$  [7]. The lithium content was determined by atomic absorption spectroscopy.

The cathode consisted of 25 mg active material and 15 mg conductive binder. The electrolyte solution was 1 M  $\text{LiPF}_6$ –ethylene carbonate (EC)/dimethylcarbonate (DMC) (1:2 in volume). Cells were usually cycled in the voltage range between 2.0 and 4.5 V at  $0.4\text{ mA}/\text{cm}^2$  (C/3). Cyclic voltammetry was carried out using a Potentiostat/Galvanostat Solartron SI-1287 at a scan rate of  $10\text{ mV}/\text{min}$ . The experiments were carried out in three-electrode glass cell. Metallic lithium was used as the counter and reference electrode.

## 3. Results and discussion

The effects of initial  $\text{LiI}/\text{MnO}_2$  molar ratio on the XRD patterns of the heated products obtained at  $200^\circ\text{C}$  are shown in Fig. 1. The symbol ● shows our orthorhombic  $\text{Li}_{0.33}\text{MnO}_2$  [4,5], which is denoted here as the orthorhombic phase (I). The symbol ○ shows crystallized orthorhombic  $\text{LiMnO}_2$  ( $a_0$ :  $2.80\text{ \AA}$ ;  $b_0$ :  $5.75\text{ \AA}$ ;  $c_0$ :  $4.58\text{ \AA}$ ) reported by Davidson et al. [12]. It is denoted here as the orthorhombic phase (II). The XRD pattern of orthorhombic phase (I) [4,5] was observed for the initial molar ratio of  $\text{LiI}/\text{MnO}_2 = 1$  (sample A). The calculated lattice parameters,  $a_0$ ,  $b_0$  and  $c_0$  of sample A are  $4.99$ ,  $9.93$  and  $2.78\text{ \AA}$ , respectively. This unit cell volume,  $137.4\text{ \AA}^3$ , is slightly higher than that of  $\text{Li}_{0.33}\text{MnO}_2$  ( $a_0$ :  $4.75\text{ \AA}$ ;  $b_0$ :  $9.81\text{ \AA}$ ;  $c_0$ :  $2.82\text{ \AA}$ ) [4,7],  $131.4\text{ \AA}^3$ , because Mn(III) having a bigger ion radius than Mn(IV) increases with the increasing in amount of intercalated Li ion in  $\text{MnO}_2$ . With the increasing initial molar ratio of  $\text{LiI}/\text{MnO}_2$ , peaks of the orthorhombic phase (II) were found in the XRD profiles, as shown in Fig. 1. In the case of the initial molar ratio of  $\text{LiI}/\text{MnO}_2 = 2.3$  (sample E), the calculated parameters of  $a_0$ ,  $b_0$  and  $c_0$  are found to be  $2.87$ ,  $5.59$  and  $4.60\text{ \AA}$ , respectively. These values are similar to the parameters of orthorhombic  $\text{LiMnO}_2$  (II) ( $a_0$ :  $2.80\text{ \AA}$ ;  $b_0$ :  $5.75\text{ \AA}$ ;  $c_0$ :  $4.58\text{ \AA}$ ). The XRD data suggest that the orthorhombic phase (I) exists at an initial molar ratio less than  $\text{LiI}/\text{MnO}_2 = 1$  and that the orthorhombic phase (II) is generated at the initial molar ratio greater than  $\text{LiI}/\text{MnO}_2 = 1.3$ .

The chemical analysis and XRD structure of the reaction products in Fig. 1, after the excess LiI in the heated products was removed, are summarized in Table 1. From the results of the chemical analysis, the chemical formula for sample A is  $\text{Li}_{0.49}\text{Mn}_{0.99}\text{O}_2$ , which means that half of the lithium ion related to the manganese ion, was incorporated into the manganese dioxides. Based on the chemical analysis, the orthorhombic phase (I) appears when the  $x$  value is less than 0.5. Samples B and C are mixtures of the orthorhombic phase (I) and the orthorhombic phase (II) as shown in Table 1. Also, the chemical formula for samples

Table 1  
Chemical analysis and XRD structure of reaction products obtained from various molar ratio of initial  $\text{LiI}/\text{MnO}_2$  at  $200^\circ\text{C}$

Initial molar ratio of $\text{LiI}/\text{MnO}_2$	Chemical analysis (mmol/g)	XRD structure
1.0 (sample A)	Li: 5.45, Mn(III): 5.01 Mn(IV): 6.01, O: 22.28	Orthorhombic (I) ( $\text{Li}_{0.49}\text{Mn}_{0.99}\text{O}_2$ )
1.3 (sample B)	Li: 6.41, Mn(III): 5.97 Mn(IV): 4.98, O: 22.12	Mixture of orthorhombic (I) and (II)
1.6 (sample C)	Li: 7.19, Mn(III): 6.31 Mn(IV): 4.54, O: 22.14	Mixture of orthorhombic (I) and (II)
1.9 (sample D)	Li: 7.77, Mn(III): 6.43 Mn(IV): 6.01, O: 22.18	Orthorhombic (II) ( $\text{Li}_{0.70}\text{Mn}_{0.97}\text{O}_2$ )
2.3 (sample E)	Li: 8.54, Mn(III): 7.67 Mn(IV): 3.07, O: 21.92	Orthorhombic (II) ( $\text{Li}_{0.77}\text{Mn}_{0.98}\text{O}_2$ )

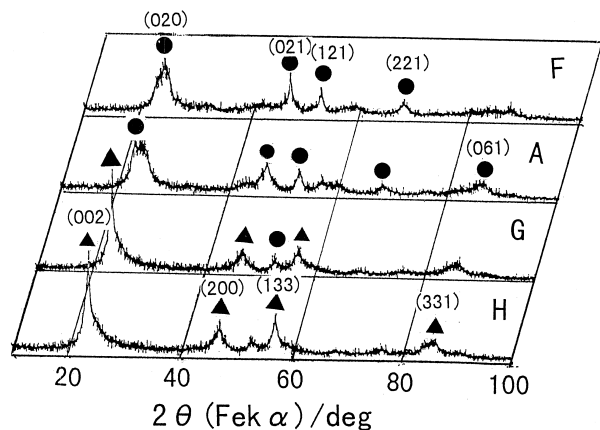


Fig. 2. XRD patterns of reaction product obtained from LiI reacting with  $\text{MnO}_2$  at initial equimolar ratio of  $\text{LiI}/\text{MnO}_2$  at (F) 150°C, (A) 200°C, (G) 250°C, and (H) 300°C. ●: Orthorhombic phase (I); ▲:  $\text{Li}_2\text{MnO}_3$ .

D and E are  $\text{Li}_{0.70}\text{Mn}_{0.97}\text{O}_2$  and  $\text{Li}_{0.78}\text{Mn}_{0.98}\text{O}_2$ , respectively. In the case of the orthorhombic phase (II), the  $x$  value in the chemical formula ( $\text{Li}_x\text{MnO}_2$ ) for samples D and E are always higher than 0.7 at the low heating temperature of 200°C. The highest value of  $x$ , 0.8, was obtained in the orthorhombic (II) structure.

The effect of heating temperature on the XRD patterns of the reaction products at the initial molar ratio of  $\text{LiI}/\text{MnO}_2 = 1$  is shown in Fig. 2. The XRD patterns of the products obtained by heating the mixture of LiI and  $\text{MnO}_2$  at 150 and 200°C (F and A in Fig. 2) confirmed the presence of the orthorhombic phase (I) (single phase). On the other hand, the peaks of  $\text{Li}_2\text{MnO}_3$  at greater than 250°C (samples G and H in Fig. 2) were confirmed at  $2\theta = 23.7^\circ, 47.0^\circ, 57.1^\circ$  and  $85.9^\circ$ . Therefore, the optimum temperature to obtain the orthorhombic phase (I) is 150–200°C.

The chemical analysis and XRD structure of the reaction products at various temperatures are summarized in Table 2. From the results of chemical analysis, the chemical formula of products obtained at 150°C (sample F), 200°C (sample A) were determined to be  $\text{Li}_{0.47}\text{Mn}_{0.98}\text{O}_2$  (orthorhombic (I), sample F) and  $\text{Li}_{0.49}\text{Mn}_{0.99}\text{O}_2$  (ortho-

rhombic (I), sample A), respectively. The highest limit in  $x$  value for the orthorhombic  $\text{Li}_x\text{MnO}_2$  (I) was determined to be essentially 0.5. Based on the chemical analysis and XRD pattern, samples G and H show a mixture of orthorhombic (I) and  $\text{Li}_2\text{MnO}_3$ .

From these results, the optimum conditions to prepare the orthorhombic phase (I),  $\text{Li}_x\text{MnO}_2$ , are an initial molar ratio  $\text{LiI}/\text{MnO}_2 = 1$  and heat treatment temperature of 150–200°C.

The relationship of the theoretical and observed capacities are summarized in Table 3. The first theoretical discharge capacity of  $\text{Li}_x\text{Mn}_y\text{O}_2$  is determined by the value of  $\text{Li}_x\text{Mn(III)}_p\text{Mn(IV)}_q\text{O}_2$  using Faraday's law. The  $q$  values of samples F and A calculated from the chemical analysis data are 0.59 and 0.54, and hence the theoretical capacities of the first discharge are 177 and 161 mA h/g, respectively. The experimental values of first discharge are 161 and 154 mA h/g for samples F and A, respectively. The first discharge capacity in the 3 V region (2.0–3.5 V) agrees with the experimental value. In the case of mixture (sample H), we tried to calculate the content of the battery inactive  $\text{Li}_2\text{MnO}_3$ . According to the chemical analysis of the Mn(IV) content, the theoretical capacity of sample H can be calculated as 227 mA h/g. The capacity difference between the theoretical and experimental values ( $227 - 132 = 95$  mA h/g) would be due to the existence of battery inactive  $\text{Li}_2\text{MnO}_3$ . This result shows that 95 mA h/g of sample H contains 41 wt.%  $\text{Li}_2\text{MnO}_3$ . Assuming that the remainder is orthorhombic (I)  $\text{Li}_x\text{MnO}_2$ , the  $x$  value can be calculated as  $\text{Li}_{0.32}\text{MnO}_2$ , which corresponds to the capacity of 207 mA h/g. Thus, we have confirmed that the calculation method of each component is possible.

The charge/discharge curves of samples A, F and H between 4.5 and 2.0 V are shown in Fig. 3. The charge/discharge curves of samples A and F (orthorhombic  $\text{Li}_x\text{Mn}_y\text{O}_2$  (I)) have two voltage plateau at ca. 2.8 and 3.5 V. The charge/discharge profile of orthorhombic (I),  $\text{Li}_{0.33}\text{MnO}_2$ , between 4.5 and 2.0 V obtained by  $\text{LiNO}_3\text{-MnO}_2$  is shown in Fig. 4. This profile agrees well with those of samples A, F and H, which show essentially the structure of the orthorhombic (I). For sample H (a mixture of orthorhombic (I) and  $\text{Li}_2\text{MnO}_3$ ), the voltage

Table 2

Chemical analysis and XRD structure of reaction products obtained from initial molar ratio  $\text{LiI}/\text{MnO}_2 = 1$  at 150°C–300°C

Heating temperature (°C)	Chemical analysis (mmol/g)	XRD structure
150 (sample F)	Li: 5.27, Mn(III): 4.38 Mn(IV): 6.62, O: 22.45	Orthorhombic (I) ( $\text{Li}_{0.47}\text{Mn}_{0.98}\text{O}_2$ )
200 (sample A)	Li: 5.45, Mn(III): 5.01 Mn(IV): 6.01, O: 22.28	Orthorhombic (I) ( $\text{Li}_{0.49}\text{Mn}_{0.99}\text{O}_2$ )
250 (sample G)	Li: 8.89, Mn(III): 1.67 Mn(IV): 8.46, O: 23.86	Mixture of orthorhombic (I) and $\text{Li}_2\text{MnO}_3$
300 (sample H)	Li: 9.92, Mn(III): 1.55 Mn(IV): 8.50, O: 23.95	Mixture of orthorhombic (I) and $\text{Li}_2\text{MnO}_3$

Table 3

Relationship of the theoretical and observed capacities

Sample	Theoretical capacity of 3 V region <sup>a</sup> (mA h/g)	First discharge capacity of 3 V region (mA h/g)
F	177	161
A	161	154
H	132 <sup>b</sup>	132

<sup>a</sup>Theoretical capacity of 3 V region is calculated as follows; cap. (3 V) =  $26.8q/F A$  h/g,  $F$  shows molecular weight.

<sup>b</sup>59 wt.% of orthorhombic (I),  $\text{Li}_{0.32}\text{MnO}_2$ : 132 mA h/g, 41 wt.% of  $\text{Li}_2\text{MnO}_3$ : 0 mA h/g.

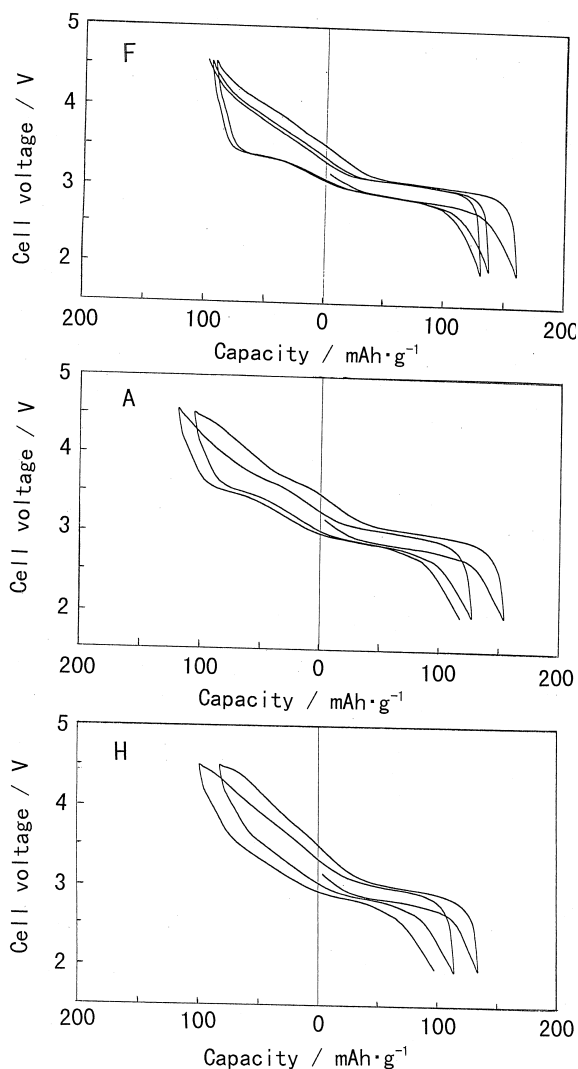


Fig. 3. Charge/discharge curves of samples A, F and H between 4.5 and 2.0 V at 0.4 mA/cm<sup>2</sup>.

plateau at 3.5 V disappears and hence the rechargeable capacity of sample H became lower than those of samples A and F. Sample A shows the highest rechargeable capacity of 250 mA h/g between 4.5 and 2.0 V. After the first

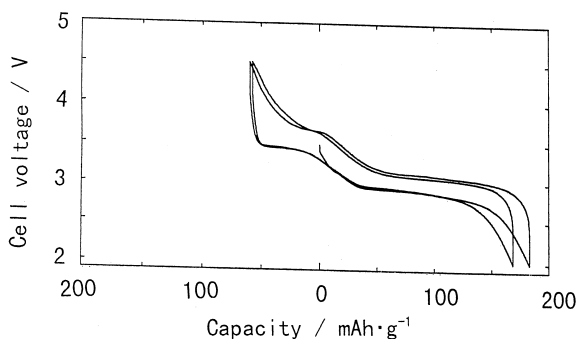


Fig. 4. Charge/discharge curve of Li<sub>0.33</sub>MnO<sub>2</sub> obtained by LiNO<sub>3</sub>-MnO<sub>2</sub> at 0.4 mA/cm<sup>2</sup>.

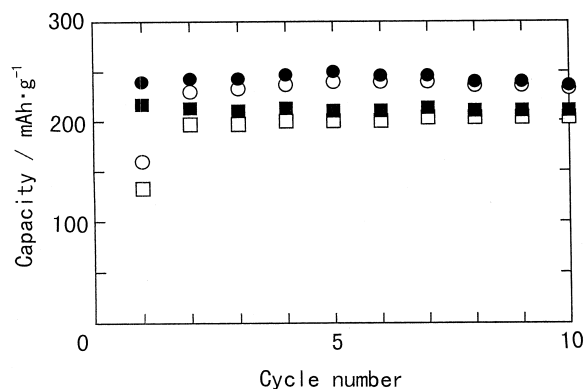


Fig. 5. Cyclic performance of samples A and H. Sample A, ●: charge; ○: discharge, sample H, ■: charge; □: discharge.

charge, the Li ion content of samples A and F remain 0.09 and 0.09 for 1 Mn in MnO<sub>2</sub>, because the first charge capacity of samples A and B are 252 and 260 mA h/g, respectively. On the other hand, the charge/discharge curve of sample E (orthorhombic (II)) is similar to the result of Davidson et al. [12] and the rechargeable capacity of it is lower than samples F and A. Therefore, the orthorhombic phase (I) is useful in comparison with orthorhombic phase (II) as a cathode for lithium batteries.

The cyclic performances of samples A and H are shown in Fig. 5. Sample A shows good cycle performance during 10 cycles and high rechargeable capacity. On the other hand, in the case of sample H, the rechargeable capacity is low as compared with sample A due to the coexistence of Li<sub>2</sub>MnO<sub>3</sub>, but the cycle performance is excellent.

A cyclic voltammogram of sample A is shown in Fig. 6. Anodic and cathodic peaks show the presence of a four step electrochemical process for lithium intercalation and deintercalation. The current efficiency is 100% because the anodic (2.15 mA h) and cathodic (2.15 mA h) capacities in the second cycle agree with each other. Therefore, this result shows that the rechargeability sample A is excellent. Peaks R and S in the reduction process correspond to the

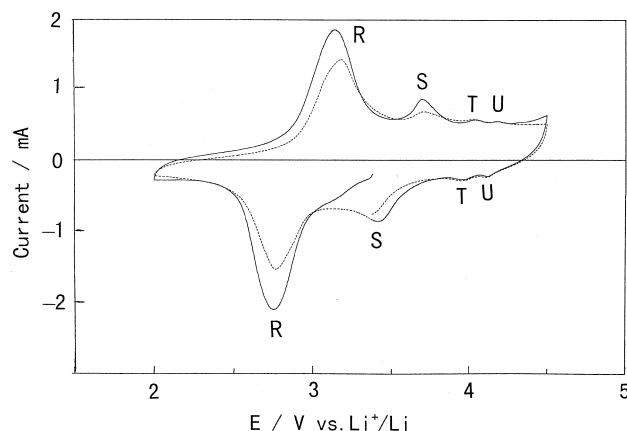


Fig. 6. Cyclic voltammogram of sample A. —: First cycle; ···: second cycle.

2.8 and 3.5 V plateaus in Fig. 3A and F, respectively. Peaks T and U are similar to the spinel  $\text{LiMn}_2\text{O}_4$ , and, hence, it is suggested that sample A contains a small amount of  $\text{LiMn}_2\text{O}_4$ .

#### 4. Conclusion

(1) We have confirmed that the battery active material of CDMO, developed by Sanyo, consist of orthorhombic (I)  $\text{Li}_{0.33}\text{MnO}_2$  and battery inactive  $\text{Li}_2\text{MnO}_3$ .

(2) The  $x$  value in  $\text{Li}_x\text{MnO}_2$  varied from 0.5 to 0.8 depending on the  $\text{LiI}/\text{MnO}_2$  molar ratio heating temperature at  $200^\circ\text{C}$ . The products are confirmed to be the orthorhombic phase (I) and orthorhombic phase (II) based on the XRD analysis. The orthorhombic phase (I) is excellent as a 3–4 V cathode material for Li batteries.

(3) The optimum conditions to prepare the orthorhombic phase (I),  $\text{Li}_x\text{MnO}_2$ , are an initial molar ratio  $\text{LiI}/\text{MnO}_2 = 1$  and heat treatment at  $150\text{--}200^\circ\text{C}$ .

(4) Charge/discharge curve of  $\text{Li}_{0.33}\text{MnO}_2$  obtained by  $\text{LiNO}_3\text{--MnO}_2$  agrees well with those of  $\text{Li}_{0.47}\text{MnO}_2$  and  $\text{Li}_{0.49}\text{MnO}_2$  which shows essentially with the orthorhombic (I) structure.

(5) The first theoretical discharge capacities of 177 and 161 mA h/g of orthorhombic  $\text{Li}_{0.47}\text{Mn}_{0.98}\text{O}_2$  (I) and  $\text{Li}_{0.49}\text{Mn}_{0.99}\text{O}_2$  (I) approximately correspond to the experimental values 161 and 154 mA h/g, respectively.

(6) The rechargeable capacity of  $\text{Li}_{0.49}\text{Mn}_{0.99}\text{O}_2$  between 4.5 and 2.0 V is ca. 250 mA h/g which corresponds to 750 W h/kg.

#### References

- [1] T. Nohma, T. Saito, N. Furukawa, H. Ikeda, J. Power Sources 26 (1989) 389.
- [2] T. Nohma, Y. Yamamoto, I. Nakane, N. Furukawa, J. Power Sources 39 (1992) 51.
- [3] A. de Kock, M.M. Rossouw, L.A. de Picciotto, M.M. Thackeray, W.I.F. David, R.M. Ibberson, Mater. Res. Bull. 25 (1990) 657.
- [4] M. Yoshio, S. Inoue, G.P. Piao, H. Nakamura, Prog. Batt. Solar Cells 9 (1990) 205.
- [5] M. Yoshio, S. Inoue, G.P. Piao, H. Nakamura, J. Power Sources 34 (1991) 147.
- [6] M. Yoshio, H. Noguchi, H. Nakamura, K. Suzuoka, Jpn. Electrochem. Soc. 64 (1996) 123.
- [7] M. Yoshio, H. Noguchi, T. Miyashita, H. Nakamura, A. Kozawa, J. Power Sources 54 (1995) 483.
- [8] Y. Xia, H. Takeshige, H. Noguchi, M. Yoshio, J. Power Sources 56 (1995) 61.
- [9] L. Li, G. Pistoia, Solid State Ionics 47 (1991) 241.
- [10] P. Dan, E. Mengeritsky, D. Aurbach, I. Weissman, E. Zinigrad, J. Power Sources 68 (1997) 443.
- [11] E. Revi, E. Teller, M.D. Levi, D. Aurbach, J. Electrochem. Soc. 145 (1998) 3440.
- [12] I.J. Davidson, R.S. McMillan, J.J. Murray, J.E. Greedan, J. Power Sources 54 (1995) 232.